

TP 13472E

**Railway Bearing Diagnostics:
Laboratory Data Analysis**

Prepared for

Transportation Development Centre
Transport Canada

By

National Research Council Canada

September 1999

TP 13472E

**RAILWAY BEARING DIAGNOSTICS:
LABORATORY DATA ANALYSIS**

by

G. Krishnappa and M. Donovan

**National Research Council Canada
Vancouver, Canada**

September 1999

This report reflects the views of the authors and not necessarily those of the Transportation Development Centre.

Since the accepted measures in the industry are imperial, metric measures are not used in this report.

Une sommaire français se trouve avant la table de matières.



1. Transport Canada Publication No. TP 13472E		2. Project No. 8886-7		3. Recipient's Catalogue No.	
4. Title and Subtitle Railway Bearing Diagnostics: Laboratory Data Analysis				5. Publication Date September 1999	
				6. Performing Organization Document No.	
7. Author(s) G. Krishnappa and M. Donovan				8. Transport Canada File No. ZCD2450-D-651	
9. Performing Organization Name and Address Innovation Centre, Manufacturing Technologies Program National Research Council Canada 3250 East Mall Vancouver, British Columbia V6T 1W5				10. PWGSC File No. Agreement	
				11. PWGSC or Transport Canada Contract No. Agreement	
12. Sponsoring Agency Name and Address Transportation Development Centre (TDC) 800 René Lévesque Blvd. West Suite 600 Montreal, Quebec H3B 1X9				13. Type of Publication and Period Covered Final	
				14. Project Officer Roy S. Nishizaki	
15. Supplementary Notes (Funding programs, titles of related publications, etc.) Co-sponsored by the Railway Safety Directorate					
16. Abstract <p>Recognizing the need for an improved wayside roller bearing defect detection system, the Association of American Railroads (AAR) implemented a research program in 1993, aimed at developing improved acoustic-based systems. In response to an invitation from the AAR, the National Research Council Canada participated in the first two phases of the program: laboratory investigations and field tests. This report describes the data analysis from the laboratory investigations to determine whether acoustic techniques can be used in wayside systems for reliable detection of faulty bearings.</p> <p>The tests were carried out using both non-defective and condemnable bearings. Acoustic signals were analysed to identify and classify defective bearings. Bearing diagnostics techniques based on pattern recognition of statistical parameters were examined. Based on the one-microphone signals, using a combination of bearing energy and impulse parameters, a pattern recognition technique to classify and identify six commonly occurring freight car bearing defects was developed. When tested, this technique successfully identified an unknown (mystery) defect. Using signals from a two-microphone configuration, a combined index method was developed. The indexes were found effective in identifying bearing defects for speed variation under constant loading. A graphic user interface system was developed based on this method.</p>					
17. Key Words Railways, cars, roller bearings, fault detectors, acoustic				18. Distribution Statement Limited number of copies available from the Transportation Development Centre	
19. Security Classification (of this publication) Unclassified		20. Security Classification (of this page) Unclassified		21. Declassification (date) —	22. No. of Pages xii, 38, app.
				23. Price Shipping/ Handling	



1. N° de la publication de Transports Canada TP 13472E		2. N° de l'étude 8886-7		3. N° de catalogue du destinataire	
4. Titre et sous-titre Railway Bearing Diagnostics: Laboratory Data Analysis				5. Date de la publication Septembre 1999	
				6. N° de document de l'organisme exécutant	
7. Auteur(s) G. Krishnappa et M. Donovan				8. N° de dossier - Transports Canada ZCD2450-D-651	
9. Nom et adresse de l'organisme exécutant Centre d'innovation, Programme des techniques de fabrication Conseil national de recherches du Canada 3250 East Mall Vancouver, Colombie-Britannique V6T 1W5				10. N° de dossier - TPSGC Accord	
				11. N° de contrat - TPSGC ou Transports Canada Accord	
12. Nom et adresse de l'organisme parrain Centre de développement des transports (CDT) 800, boul. René-Lévesque Ouest Bureau 600 Montréal (Québec) H3B 1X9				13. Genre de publication et période visée Final	
				14. Agent de projet Roy S. Nishizaki	
15. Remarques additionnelles (programmes de financement, titres de publications connexes, etc.) Recherche coparrainée par la Direction générale de la sécurité ferroviaire					
16. Résumé <p>Reconnaissant le besoin d'un système amélioré de détection en bordure de voie des roulements défectueux, l'AAR (Association of American Railroads) a lancé en 1993 un programme de recherche axé sur le développement de systèmes acoustiques. Invité par l'AAR, le Conseil national de recherches du Canada a participé aux deux premières phases du programme : les expériences en laboratoire et les essais sur le terrain. Ce rapport présente l'analyse des données issues des expériences en laboratoire, qui visait à déterminer si la détection acoustique en bordure de voie était réalisable et donnerait des résultats fiables.</p> <p>Le protocole d'essai prévoyait le contrôle aussi bien de roulements en bon état que de roulements à réformer. L'analyse des signaux acoustiques visait à repérer les roulements défectueux et les classer par type de défaut. Les chercheurs ont également examiné des techniques de diagnostic fondées sur l'analyse typologique de paramètres statistiques. Partant de signaux obtenus par microphone unique, ils ont mis au point une technique d'analyse typologique permettant de repérer et de différencier six défauts courants chez les roulements de bogies marchandises. Lors des essais, cette technique a permis d'identifier un défaut «mystère», c'est-à-dire un défaut dont on ne connaissait pas la nature en partant. Des signaux acquis au moyen de deux microphones ont débouché sur une méthode à indices composites. Cette méthode a permis de reconnaître les défauts dans des conditions de vitesse variable et charge constante. Un système à interface utilisateur graphique fondé sur cette méthode a été mis au point.</p>					
17. Mots clés Chemins de fer, wagons, roulements, détecteurs de défauts, acoustique			18. Diffusion Le Centre de développement des transports dispose d'un nombre limité d'exemplaires.		
19. Classification de sécurité (de cette publication) Non classifiée		20. Classification de sécurité (de cette page) Non classifiée		21. Déclassification (date) —	22. Nombre de pages xii, 38, ann.
					23. Prix Port et manutention

Executive Summary

Defective bearings cause many accidents affecting the safety of railway operations. The railway industry is concerned with reliable methods for wayside monitoring of wheel axle bearings in moving freight cars. Recognizing the need for an improved wayside monitoring system, the Association of American Railroads (AAR) embarked on the Improved Wayside Research Project in 1993. AAR invited all parties interested in developing a better system with improved detection accuracy. At the invitation of AAR, NRC's Innovation Centre participated in the test program with the intention of developing techniques to identify and classify bearing defects, eventually leading to a commercial system. The Transportation Development Centre provided partial program funding for 1996-98.

The AAR Wayside Railway Bearing Detection Program comprised two phases:

- Laboratory investigation to determine whether acoustic techniques can be reliably used in wayside fault detection.
- Field tests using a moving test train composed of a locomotive and several test cars with defective bearings to identify the defects investigated in the laboratory.

This report describes the data analysis from the first phase's laboratory investigations. The tests were carried out at the AAR Transportation Test Facility in Pueblo, Colorado, from December 1995 to April 1996, using the AAR roller bearing test rig. A set of baseline measurements was obtained using a bearing with no defects, prior to testing with defective bearings. Several bearings with known faults were tested at speeds and loads typically experienced by bearings in moving freight cars. The faulty bearings included condemnable ones with single cup spall, multiple cone spall, water etching, multiple cup spall, multiple cone spall, and some remanufactured bearings. A mystery bearing was included in the tests to validate the techniques in diagnosing unknown faults.

Acoustic signals were recorded in two directions, using two microphones close to the test rig, mounted at 45 degree angles to each other. This arrangement covers an extended range of wheel rotation, anywhere from 0.5 to 1.0 rotation of the wheel, depending on the speed of the train.

A bearing diagnostic method based on pattern recognition of statistical parameters was investigated. This method was based on one-microphone signals. Using a combination of bearing acoustic signal energy and impulse parameters, techniques to classify and identify six commonly occurring freight car bearing defects were developed. The six statistical parameters considered were peak, rms, crest factor, Kurtosis, impulse factor, and shape factor. Using trend analysis, the dimension of the feature space was reduced to two vectors, a

combination of the six parameters. When tested, this technique successfully identified the unknown (mystery) defect.

Using signals from the two-microphone arrangement, a combined index method was developed to identify bearing defects. A linear model to calculate an index consists of the sum of the two amplitudes of the defect frequency and their correlation coefficient. For the purpose of increasing the clustering effect of each defect under different operating conditions, the weighting factors were determined by using the intraclass transformation. The combined index method was used to diagnose the defects of the roller bearings from the data obtained from the laboratory tests. Five classes of bearing conditions were considered: the good bearing, and those with single cone spall, single cup spall, multiple cup spall, and a broken roller.

A graphic interface based on the combined index method was developed. It provides the capability to capture microphone signals and store them in ASCII or binary files. The user can then perform individual statistical and signal analysis functions on the acoustic data or run them through a bearing diagnostics algorithm. The bearing diagnosis will highlight the most likely defect exhibited by the bearing.

To develop a viable commercial system, further work is required to examine these techniques using field data.

Sommaire

Les roulements défectueux sont à l'origine de nombreux accidents ferroviaires. L'industrie du transport ferroviaire cherche des moyens fiables de détection des paliers d'essieux défectueux, utilisables en bordure de voie pour repérer les wagons à risque. Reconnaisant le besoin d'un système amélioré de détection en bordure de voie des roulements défectueux, l'AAR (Association of American Railroads) a lancé en 1993 un programme de recherche axé sur le développement de systèmes acoustiques. Cette association a invité à participer à son programme toutes les parties intéressées au développement d'un système perfectionné à capacité de détection précise améliorée. Le Centre d'innovation du Conseil national de recherches du Canada a participé au programme d'essais, visant à mettre au point des techniques de repérage et de classification des roulements défectueux que l'on pourrait éventuellement intégrer à un système opérationnel. Le Centre de développement des transports a contribué au financement des travaux entre 1996 et 1998.

Le Wayside Railway Bearing Detection Program (Programme de recherche sur la détection en bordure de voie des roulements défectueux) de l'AAR comprenait deux phases :

- Une phase d'expérimentations en laboratoire destinées à déterminer si la détection acoustique en bordure de voie était réalisable et donnerait des résultats fiables.
- Une phase d'essais sur le terrain mettant en oeuvre un train formé d'une locomotive et de plusieurs wagons équipés de roulements défectueux et visant à repérer les défauts étudiés en laboratoire.

Ce rapport présente l'analyse des données issues des expériences en laboratoire menées au cours de la phase I. Les essais ont été réalisés au Transportation Test Facility de l'AAR à Pueblo, Colorado, entre décembre 1995 et avril 1996, au moyen du banc d'essais de roulements qui s'y trouve. On a d'abord obtenu une série de données de référence caractérisant un roulement en bon état, avant de passer aux essais avec roulements défectueux. Ainsi, plusieurs roulements présentant des défauts connus ont été soumis à des vitesses et charges représentatives des conditions rencontrées en service marchandises normal. Les roulements défectueux comprenaient des roulements à réformer qui présentaient un écaillage localisé sur bague extérieure, un écaillage multipoints sur bague intérieure, des traces de corrosion, un écaillage multipoints sur bague extérieure, ainsi que quelques roulements réusinés. Un roulement «mystère» a été intégré aux essais pour vérifier si la technique permettait de reconnaître des défauts inconnus.

Les signaux acoustiques ont été enregistrés de deux points différents, au moyen de deux microphones disposés à proximité du banc d'essai, à 45 degrés l'un par

rapport à l'autre. Ce montage permet de contrôler une plage étendue de rotation des roues, allant de 0,5 rotation à un tour complet, selon la vitesse du train.

Les chercheurs ont étudié une méthode de diagnostic des roulements fondée sur une analyse typologique de différents paramètres statistiques. Cette méthode exploite des signaux enregistrés par un seul microphone. Partant d'une combinaison de signaux d'énergie acoustique et de paramètres d'impulsion, les chercheurs ont mis au point des techniques d'identification et de différenciation de six défauts courants sur les roulements de bogies marchandises. Les six paramètres statistiques retenus étaient les valeurs maximales, les valeurs efficaces, les facteurs de crête, l'aplatissement, les coefficients d'impulsion et les coefficients de forme. Une analyse de tendances a permis de réduire l'espace des attributs à deux vecteurs, soit une combinaison des six paramètres. À l'expérimentation de cette technique, les chercheurs ont réussi à identifier le défaut «mystère», dont la nature était inconnue.

À l'aide des signaux provenant du montage à deux microphones, les chercheurs ont par la suite développé une méthode d'identification des défauts de roulements faisant appel à des indices composites. Un modèle linéaire utilisé pour calculer un indice composite repose sur la somme des deux amplitudes de la fréquence caractéristique du défaut et sur leur coefficient de corrélation. Afin d'accentuer l'effet de regroupement de chaque défaut dans différentes conditions de fonctionnement, les coefficients de pondération ont été déterminés par transformation intra-classe. La méthode à indices composites a été mise en oeuvre pour diagnostiquer les défauts des roulements à partir des données issues des essais en laboratoire. Cinq classes d'état ont été prises en compte : un roulement sain, des roulements présentant un écaillage localisé de la bague intérieure, un écaillage localisé de la bague extérieure ou un écaillage multipoints de la bague extérieure, ainsi qu'un roulement ayant un rouleau cassé.

Les chercheurs ont mis au point une interface utilisateur graphique, fondée sur la méthode à indices composites, qui permet de capter les signaux acoustiques et les conserver dans des fichiers ASCII ou binaires. L'utilisateur peut alors soumettre les données acoustiques à différentes analyses statistiques ou différents traitements du signal, isolément, ou encore alimenter un algorithme de diagnostic. Cet algorithme mettra en évidence le défaut le plus probable du roulement.

Pour arriver à mettre au point un système opérationnel viable, il faudra étudier plus avant ces techniques en utilisant des données acquises sur le terrain.

CONTENTS

1	Introduction	1
2	Overview of Freight Car Bearing Assembly	3
3	AAR Test Plan	4
4	Laboratory Investigations	5
5	Bearing Diagnostics Techniques Using Vibration and Acoustic Analysis	7
6	Pattern Recognition of Statistical Parameters	8
6.1	Rudiments of Pattern Recognition	8
6.1.1	Pattern Space	9
6.1.2	Feature Space	11
6.1.3	Classification Space	11
7	Analysis of Data Based on One-Microphone Signals	12
7.1	Selection of Pattern Space	12
7.2	Trend Analysis	13
7.3	Selection of Feature Space	14
7.4	Intraclass Transformation	15
7.5	Formation of Classification Space	16
8	Bearing Diagnostics and Classification Based on One-Microphone Signals	18
9	Combined Index Method Using Two-Microphone Signals	19
9.1	Determination of Weighting Factors	19
10	Bearing Diagnosis Using Combined Index Method	22
10.1	Prototype Data Processing	22
10.2	Weighting Factors Considering Speed Variation	22

10.3	Weighting Factors Considering Load Variation	24
10.4	Graphic User Interface	25
11	Conclusions	26
	Figures	27
	References	38
	Appendix A: Test Set-Up and Instrumentation	

LIST OF FIGURES

Figure

1	Freight Car Bearing Assembly.	27
2	Bearing Test Rig.	27
3	Two-Microphone Measurement System.	28
4	Single Cup Spall	28
5	Multiple Cone (inner race) Spalling	28
6	Water Etching	29
7	Multiple Cup (outer race) Spalling	29
8	Broken Roller	30
9	Single Cone Spall	30
10	Spun Cone.	31
11	Mathematical Transformations of Four Spaces	31
12a	Variation of the Four Parameters, z_3 to z_6 , with Speed for Light Loading.	32
12b	Variation of the Four Parameters with Speed for Heavy Loading	32
13	Feature Space without Intra-class Transformation.	33
14	Feature Space with Intra-class Transformation	33
15	Classification Space	34
16	Identification of Unknown Bearing Fault	34
17	Index of Different Defect Classes under the Constant Sum Constraint	35
18	Index Overlapping between Different Defect Classes	35
19	Index of Different Defect Classes under the Volume Constraint	36

20	Index of Different Defect Classes Considering Two Loading Conditions	36
21	Index of Different Defect Classes Based on the Covariance of Two Loading Conditions	37
22	Picture of the Developed Software.	37

LIST OF TABLES

Table

1	Defect Signals from CD #1	5
2	Defect Signals from CD #2	6
3	Summary of Trend Analysis	14
4	Bearing Damage Conditions	18
5	Prototype for Good Bearing	22
6	Prototypes for the Single Cone Spall	23
7	Prototypes for the Single Cup Spall	23
8	Prototypes for the Multiple Cup Spall	23
9	Prototypes for the Broken Rollers.	23
10	Weighting Factor under the Constant Sum Constraint	24
11	Weighting Factors Considering Two Different Loading Conditions	25
12	Weighting Factors Based on the Covariance of Two Loading Conditions	25

RAILWAY BEARING DIAGNOSTICS: LABORATORY DATA ANALYSIS

1.0 Introduction

Defective bearings cause many accidents affecting the safety of railway operations. Consequently the railway industry is concerned with reliable methods for wayside monitoring of wheel axle bearings in moving freight cars. The alarm accuracy of the two existing wayside monitoring systems, "hot bearing detector" (HBD) and "acoustic bearing detector" (ABD), is unsatisfactory. Both systems are giving many false alarms resulting in costly removal of the bearings without the need for a safety improvement. The HBD uses wayside infrared transducers to monitor bearing temperatures as the train passes by the detector by intercepting a portion of the infrared radiation from each bearing. It issues an alarm if the bearing exceeds the preset user-programmable limits. The ABD is designed to detect bearing flaws before the overheated condition occurs, using wayside microphones to monitor acoustic radiation from the train as it passes.

Recognizing the need for an improved wayside monitoring system, the Association of American Railways (AAR) embarked on the Improved Wayside Research Project in 1993. They invited all participants who were interested in developing a better system with improved detection accuracy. At the invitation of AAR, NRC's Innovation Centre participated in the first two phases of the test program with the intent of developing techniques to identify and classify bearing defects leading to a commercial system. The Transportation Development Centre provided partial program funding for 1996-98.

Initially, the AAR Wayside Railway Bearing Detection Program was comprised of two phases:

- Laboratory investigation to determine whether acoustic techniques can be reliably used in wayside bearing fault detection.
- Field tests using a moving test train composed of a locomotive and several test cars with defective bearings to identify the defects investigated in the laboratory phase.

The tests of both phases of the program were carried out at the AAR Transportation Test Facility in Pueblo, Colorado. Using a wheel axle bearing test rig, the laboratory tests were carried out during 1995-96 on condemnable defective bearings that were removed from operating cars in service. The field test phase of the program was implemented during the summer of 1997. Based on the success of these tests, in February 1998, AAR arrived at a plan for the third phase of the program to be implemented in the summer/fall 1998. The tests under this program are aimed at examining the possibility of reliably using the proposed acoustic techniques in a simulated revenue service. These tests also

provide an opportunity to conduct more experiments with additional instrumentation to acquire acoustic signals for further development of the techniques.

During the two years 1996-98, with funding support from TDC, NRC's Innovation Centre developed signal processing and analysis techniques to detect and classify bearing faults based on the laboratory test data under AAR Phase I program, and developed some very limited analysis techniques for the track data under Phase II.

2 Overview of Freight Car Bearing Assembly

The most common bearing configuration found in North American freight cars today is the grease lubricated, double row tapered type, as shown in Figure 1. The stationary raceways are located in the outer ring, which is commonly referred to as the “cup”. The rotating raceways are located in the inner ring, and are referred to as “cones”. The roller elements ride on the rotating raceways, and the cage assembly separates each roller element from its adjacent rollers. The cone diameter is manufactured to be 0.0025 inch to 0.0045 inch smaller than the axle journal, which results in an interference fit between the cones and the journal when the bearing is mounted. The two cones are separated by a spacer ring, which sets the amount of bearing endplay. Two grease seals, which press into the cup and ride on the wear rings, act to retain the bearing lubricant and prevent lubricant contamination. The bearing is held on the main axle journal by an end assembly, which includes three cap screws.

3 AAR Test Plan

In 1993, AAR, under contract from the Federal Railroad Administration, invited all interested participants to discuss their test plans for developing a reliable system of wayside monitoring of wheel axle bearings using acoustic techniques. They provided an overview of the railroad bearing design, defect classification, failure mechanisms, and current defective bearing wayside techniques employed by the railroad industry.

The two mechanisms believed to cause the majority of bearing failures are cone slippage and bearing seizure. Cone slippage occurs when the interference between the cone bore and the axle journal becomes degraded due to a variety of factors. Bearing seizures occur when the rotating and stationary raceways become locked together.

The AAR's program objectives were:

- define the capabilities of the current acoustic bearing technology,
- conduct laboratory and on-track tests to determine whether acoustic techniques can be reliably used to identify the following conditions:
 1. spun cone condition in the absence of spalling
 2. broken roller element
 3. broken cage condition
 4. AAR condemnable cone spall defect
 5. AAR non-condemnable cone spall defect
 6. AAR condemnable cup spall defect
 7. AAR non-condemnable cup spall defect
 8. AAR condemnable cup Brinell defect
 9. AAR non-condemnable cup Brinell defect
- conduct laboratory and on-track tests to identify improvements to acoustic signal processing currently in use and to determine improved processing techniques,
- develop an outline for investigating alternative strategies or techniques to identify such defective frequencies should acoustic techniques be unable to detect any of the above defective conditions.

The program objectives were to be addressed in three separate subtasks:

- Subtask A – laboratory investigations
- Subtask B – on-track investigations
- Subtask C – alternative method of investigation

Subtask A is discussed in section 4.

4 Laboratory Investigations

The objective of the laboratory investigations was to evaluate the feasibility of using acoustic detection techniques to identify bearing defects. A set of baseline measurements was to be obtained using a bearing with no defects prior to conducting the tests with defective bearings.

The laboratory tests were conducted at the AAR Transportation Test Facility in Pueblo, Colorado, during December 1995-April 1996. The tests were carried out using the roller bearing test rig shown in Figure 2.

The various details pertaining to test set-up and instrumentation details are given in Appendix 1. The loads on the test bearings corresponded to those carried by the freight car during its operations, namely 8K, 27K, and 33K lb. The laboratory tests included 15 separate bearings tested at speeds corresponding to 25, 30, 40, 50, 60, 70, and 80 mph. Bearings were run up and down over the speed range. Acoustic signals were recorded in two directions by using two microphones mounted at 45° angles to each other, as shown in Figure 3.

For the track investigation, a similar two-microphone arrangement will cover an extended range of wheel rotation. This may vary anywhere from 0.5 to 1.0 rotation of the wheel, depending on the speed of the train.

The test bearings with the various examined defect conditions are listed in Tables 1 and 2.

Table 1. Defect Signals from CD #1

Test Number (CD#1)	Defect (Class F bearings)
1.	Remanufactured 'good bearing'
2.	Condemnable single cup spall
3.	Condemnable multiple connecting cone spall
4.	Condemnable water etching
5.	Condemnable multiple connecting cup spall
6.	Broken roller
7.	Mystery bearing (blind test sample bearing)

Table 2. Defect Signals from CD #2

Test Number (CD#2)	Defect (Class E bearings)
1.	Remanufactured 1/8 inch cup spall
2.	Condemnable multiple connecting cone spall
3.	Condemnable water etching
4.	Remanufactured good bearing
5.	Small repaired single cup spall
6.	Single cone spall
7.	Simulated broken roller in outboard cone
8.	Mystery bearing (blind test sample bearing)

Figures 4 to 10 show the photographs of defective bearings.

5 Bearing Diagnostics Techniques Using Vibration and Acoustic Analysis

The subject of roller bearing diagnostics has been studied over the last twenty-five years because they are used in all rotating machinery from small to large size (Rao, 1996). Common failures of bearing assemblies include spalling, corrosion, and brinelling. These defects induce repetitive vibrations when roller bearing elements encounter them (McFadden and Smith, 1984a,b.) The objective of bearing diagnostics is to identify the type of defects using the technologies that measure and process these defect-induced vibration signals.

Vibration analysis is a reliable technique that is used extensively for condition monitoring and diagnostics by the users and operators of machinery. Vibrating surfaces generate sound; therefore, diagnostic techniques developed for vibration signals are equally applicable for acoustic signals. Most bearing monitoring techniques involve significant signal processing and analysis to extract the characteristics of the signals associated with various conditions of the machinery. Analyses can be performed in the time domain, frequency domain, or time-frequency domains. Through time domain analysis, statistical parameters, such as peak levels, rms, crest factor, kurtosis, impulse factor, and shape factor (Howard, 1994) can be calculated and compared. Frequency domain analysis or spectrum analysis, transforms the time-domain data into the frequency domain and makes comparisons of the results at known defect frequencies. Other analysis methods incorporating elements of frequency domain analysis include envelope analysis and cepstrum analysis. Time-frequency domain analysis is used for processing transient and non-stationary signals using the short-time Fourier transform, Wigner-Ville distribution, and wavelets.

In practice, spectrum analysis is the most common method, used with trend analysis, for bearing diagnostics. This method detects the frequencies of the repetitive impulses generated by the bearing defects. The method is effective for detecting single defects which exhibit distinct defect frequencies. However, it becomes less effective when defect frequencies are not distinct, as is the case with multiple defects. Time domain analysis may overcome this weakness of spectrum analysis, as statistical parameters can provide information such as the shape of the amplitude probability distribution and the energy level of the vibration signals. Much research (Braun, 1986; Howard, 1994; and Rao, 1996) has been done using these parameters individually to detect the bearing defects, and the results have shown that each parameter is only effective for certain defects. For example, spikiness of vibration signals, indicated by crest factor and kurtosis, implies incipient defects, while the rms and peak parameters indicate the high energy levels associated with severe defects.

6 Pattern Recognition of Statistical Parameters

An intuitive idea is to combine the six common statistical parameters mentioned above into a weighted index to differentiate between different defects (classes of data). The pattern recognition problem can be described as transformations of four spaces, namely from the *measurement space*, to the *pattern space*, to the *feature space*, and finally, to the *classification space*. Successive transformations accentuate the differences between the classes and make the results more readable. Based on trend analysis of the statistical parameters, some or all of them can be selected to form a pattern space. A feature space is then formulated by a nonlinear transformation from the pattern space, and it has dimension of two for the purpose of displaying the results on a plane. The intraclass transformation can also be used at this point to cluster the data of different bearing defects into different regions. Classification of bearing defects is done by the discriminant function, which is generated through a supervised learning process. The discriminant function relates different bearing defects to different regions in the classification space. Testing the proposed method involves first training the classification space using the data from the bearings with known seeded defects and then using the classification space to diagnose the unknown bearings.

6.1 Rudiments of Pattern Recognition

The subject of pattern recognition may be briefly stated as the identification of classifiable patterns from measurement data. This subject has been studied for many years in different applications, and the methods in the literature can be categorized as *heuristic*, *linguistic*, and *mathematic* (Andrews, 1972.) The technique adopted in this paper is the latter. In this section, the rudiments of mathematical pattern recognition are discussed. The reader can refer to the book by Andrews (1972) for details.

As illustrated in Figure 11, we describe the mathematical pattern recognition as identifying classifiable patterns through mathematical transformations of four spaces: measurement space, M , to the pattern space, P , to the feature space, F , and finally, to the classification space, C .

$$M \rightarrow P \rightarrow F \rightarrow C$$

Note that this description is different from that given by Andrews (1972) in that the measurement space is included. As will be discussed in the following subsection, this allows construction of the pattern space by means of some analysis methods, such as statistics, rather than just using the measured data.

The measurement space is constructed from measurement data and its dimension is denoted by N , so we consider the following column data vector

$$\mathbf{s} = [s_1, s_2, \dots, s_i, \dots, s_N]^T$$

i.e. a digitized data sample with N data points. Hence the measurement space is formed by N axes and a vector \mathbf{s} represents a point in the space. To establish the classifiable patterns, learning techniques should be applied. The one adopted here is supervised learning, which uses prototype data for each class that we wish to identify to establish classifiable patterns. For each class, we may need a set of prototype data vectors. So the data vector of the m th prototype corresponding to class k is expressed as

$$\mathbf{q}_m^{(k)} = [q_{1m}^{(k)}, q_{2m}^{(k)}, \dots, q_{Nm}^{(k)}]^T$$

where $m = 1, \dots, M_k$ and M_k denotes the number of prototype data vectors for the k th class. Given K classes, the total number of data sets, N_d , is given as

$$N_d = \sum_{k=1}^K M_k \quad (1)$$

6.1.1 Pattern Space

According to Andrews (1972), the pattern space was simply represented by measurement data. We extend this so that it can be defined by certain methods of analysis such as statistics. Therefore, after this process, the data vector, \mathbf{s} , will become the following new vector

$$\mathbf{x}_p = [x_{p1}, x_{p2}, \dots, x_{pi}, \dots, x_{pR}]^T$$

where the subscript p indicates the pattern space. The dimension of the pattern space is denoted by R , where $R \leq N$. A prototype in the pattern space is given by the following vector.

$$y_{pm}^{(k)} = [y_{p1m}^{(k)}, y_{p2m}^{(k)}, \dots, y_{pRm}^{(k)}]^T$$

The problem with pattern recognition lies in correctly classifying the known prototypes and acquiring some degree of confidence based on certain criteria. The solution is based on the assumption that the pattern space forms a metric space that satisfies the following conditions (Andrews, 1972):

1. $d(\mathbf{a}, \mathbf{b}) = d(\mathbf{b}, \mathbf{a})$
2. $d(\mathbf{a}, \mathbf{b}) \leq d(\mathbf{a}, \mathbf{c}) + d(\mathbf{b}, \mathbf{c})$
3. $d(\mathbf{a}, \mathbf{b}) \geq 0$
4. $d(\mathbf{a}, \mathbf{b}) = 0$ iff $\mathbf{a} = \mathbf{b}$

where d denotes a distance function, and \mathbf{a} , \mathbf{b} , and \mathbf{c} represent three vectors in the pattern space. In terms of the metric space, the similarity of a point x_p to the k th class can be measured by

$$S(x_p, \{y_{pm}^{(k)}\}) = \frac{1}{M_k} \sum_{m=1}^{M_k} d^2(x_p, y_{pm}^{(k)}) \quad (2)$$

This similarity measure is an average of the squared distance between the point \mathbf{x} and the set of prototypes, $\mathbf{y}_{pm}^{(k)}$. To ensure that we compare vectors with the same unit, normalization of measurement data is required, which is referred to as squaring up the pattern space. A simple way to do this is to divide the measurement data by its variance, known as variance normalization.

6.1.2 Feature Space

The feature space is the intermediate domain between the pattern space and the classification space, with its dimension denoted as L . The data vector \mathbf{x}_f and the prototype vector $\mathbf{y}_{fm}^{(k)}$ in the feature space are defined as

$$\mathbf{x}_f = [x_{f1}, x_{f2}, \dots, x_{fi}, \dots, x_{fL}]^T$$

and

$$\mathbf{y}_{fm}^{(k)} = [y_{f1m}^{(k)}, y_{f2m}^{(k)}, \dots, y_{fLm}^{(k)}]^T$$

where the subscript f denotes feature space.

This space has a reduced dimension that serves two purposes. First, a classification algorithm can be efficiently computed and the results readily presented. Second, classification characteristics can be extracted. The process of selecting a feature space involves finding a transformation, either linear or nonlinear, to reduce the dimension of the pattern space yet maintain discriminatory characteristics for classification purposes. There are a number of transformation methods. The one adopted in the paper is the intraclass transformation, which will be discussed later.

6.1.3 Classification Space

The classification space is essentially the feature space but with separating surfaces introduced between classes. The classification algorithm defines the space partitions in the L dimensional feature space, with each disjoint region being associated with one class. For K classes, there will be $K-1$ separating surfaces, and for an L dimensional feature space, these surfaces are hyperplanes with $L-1$ dimension(s). The separation is a point on a line for $L=1$, a line on a plane for $L=2$, and a plane in a volume for $L=3$. Since the data is usually not linearly separable, space partition generally results in nonlinear surfaces. For example, the boundaries in the classification space for $L=2$ may be formed by curves.

7 Analysis of Data Based on One-Microphone Signals

Pattern recognition analysis was done on the one-microphone signals. The raw data is a series of numbers representing the amplitude of signals at discrete times. The first step in the analysis is to construct the pattern space based on a statistical analysis of the signals (the measurement space). In sub-section 7.1 we describe how to select the statistical parameters to form the pattern space. In addition, this section describes the selection and formation of feature space and classification space.

7.1 Selection of Pattern Space

Six commonly used statistical parameters for bearing diagnosis (Howard, 1994) are Peak, RMS, CrestFactor, Kurtosis, ImpulseFactor, and ShapeFactor, which are considered here to form the pattern space. In terms of the sampling data vector, \mathbf{s} , these parameters can be defined as follows:

$$Peak = \frac{1}{2} (\max(s_i) - \min(s_i)) \quad (3)$$

$$RMS = \sqrt{\frac{1}{N} \sum_{i=1}^N (s_i - \bar{s})^2} \quad (4)$$

$$CrestFactor = \frac{Peak}{RMS} \quad (5)$$

$$Kurtosis = \frac{\frac{1}{N} \sum_{i=1}^N (s_i - \bar{s})^4}{RMS^4} \quad (6)$$

$$ImpulseFactor = \frac{Peak}{(1/N) \sum_{i=1}^N |s_i|} \quad (7)$$

and

$$ShapeFactor = \frac{RMS}{(1/N) \sum_{i=1}^N |s_i|} \quad (8)$$

where \bar{s} denotes the mean value of the time domain signal.

It has been shown in the literature (Howard, 1994) that Peak and RMS values directly reflect the energy level of the vibration signals. Since the localized bearing defects result in structural vibrations, these two parameters are generally used to indicate the presence and severity of the defects. CrestFactor and Kurtosis are less dependent on the vibration level but are sensitive to the spikiness of the vibration signals. As such, they can provide early indication of significant changes in the vibration signals. However, as the damage increases, the vibration signals become more random, and the values of CrestFactor and

Kurtosis can decrease to the undamaged level. ImpulseFactor and ShapeFactor have similar properties to those of CrestFactor and Kurtosis.

Note that Peak and RMS have a unit, while the other four parameters are dimensionless. As the normalization factor for these two parameters, we used the RMS value of the undamaged bearing data, denoted by RMS_o . Its calculation considered all possible loads and rotating speeds for the bearing under study. Through our experiments, we found that RMS_o can improve the robustness of the energy level parameters (Peak and RMS) against variation in the bearing operating conditions. In terms of RMS_o we can rewrite eqns. (3) to (8) and define the following normalized vector \mathbf{z} .

$$\mathbf{z} = \begin{bmatrix} z_1 \\ z_2 \\ z_3 \\ z_4 \\ z_5 \\ z_6 \end{bmatrix} = \begin{bmatrix} Peak / RMS_o \\ RMS / RMS_o \\ CrestFactor \\ Kurtosis \\ ImpulseFactor \\ ShapeFactor \end{bmatrix} \quad (9)$$

7.2 Trend Analysis

Since the statistical parameters of bearing vibration signals are affected by the bearing operating conditions, e.g. the rotating speed and load, trend analysis is conducted to investigate the effect of these operating conditions on the statistical parameters. We intend to use the two energy level parameters, z_1 and z_2 , while examining the similarity among the other four parameters z_3 to z_6 , which pertain to spikiness.

Figure 12(a) shows the variation of the four parameters, z_3 to z_6 , with the rotating speed for light loading, and Figure 12(b) shows this variation for heavy loading. In the figures, the lines with “*” represent the undamaged bearings while the lines with “+” represent bearings with a single spall on the outer race. It can be observed from Figure 12(a) that CrestFactor and Kurtosis have a similar trend; whereas ImpulseFactor and ShapeFactor share another similar trend. Furthermore, these parameters are calculated for the same bearings under two different loads, and Figure 12(b) shows that all four parameters have a similar trend corresponding to the different loading conditions under the same speed. A similar trend was found in our study for other types of bearing defects. Table 3 summarizes the trend analysis.

Table 3. Summary of Trend Analysis

Variable	Speed	Load
Z ₃	+	*
Z ₄	+	*
Z ₅	#	*
Z ₆	#	*

+, #, and * indicate the similarity

Based on the trend analysis, we choose Kurtosis (z₄) against CrestFactor (z₃), and ImpulseFactor (z₅) against ShapeFactor (z₆.) Note that Peak/RMS_o (z₁) is similar to CrestFactor, and based on our numerical experiment, we use the latter instead of the former. Hence, we define the following vector \mathbf{x}_p to form the pattern space

$$\mathbf{x}_p = \begin{bmatrix} x_{p1} \\ x_{p2} \\ x_{p3} \\ x_{p4} \end{bmatrix} = \begin{bmatrix} RMS / RMS_o \\ Kurtosis \\ CrestFactor \\ ImpulseFactor \end{bmatrix} \quad (10)$$

The dimension of our pattern space is four, i.e. R=4.

7.3 Selection of Feature Space

Probably the most important aspect of pattern recognition is the selection of the feature space. Proper and efficient feature extraction allows large dimension reduction yet, as much as possible, retains the useful information. Constructing a feature space so that the data form a planar image is especially advantageous, because a planar image can be readily perceived and analyzed by a human observer. Consequently, it is desirable to extract two indices from our aforementioned four parameters.

We consider two key characteristics that statistical parameters might give us about the bearing vibration signals. One is the spikiness and the other is the energy including the shape of the amplitude distribution density and the energy level of the vibration. The first is straightforward and can be provided by Crest Factor, Kurtosis, or Impulse Factor. We choose Kurtosis in view of its robustness against variation with the operating conditions, as indicated in Figures 10(a) and 10(b). Based on the studies reported in the literature (Howard, 1994), the shape of the amplitude density distribution can be reflected by the statistical parameters pertinent to the impulsiveness of the signal, that is, CrestFactor, Kurtosis, and ImpulseFactor. Therefore, the second feature, with some trial and error, is selected as:

$$\frac{RMS}{RMS_0} \cdot \frac{CrestFactor}{Kurtosis} + ImpulseFactor \quad (11)$$

By substituting eqn. (5) for Crest Factor into eqn. (11) and using a logarithmic scale for the second feature, the vector defining the feature space is given as

$$\mathbf{x}_f = \begin{bmatrix} x_{1f} \\ x_{2f} \end{bmatrix} = \left[\log \left(\frac{Kurtosis}{RMS_0 \cdot Kurtosis} + ImpulseFactor \right) \right] \quad (12)$$

The dimension of our feature space is two, i.e. $L=2$. Accordingly, the prototype vector representing a sample for the k th class of bearing defect is defined as

$$\mathbf{y}_{fm}^{(k)} = \begin{bmatrix} y_{f1m}^{(k)} \\ y_{f2m}^{(k)} \end{bmatrix} \quad (13)$$

Note that the actual statistical parameters used in the computation of our approach are Peak, RMS_0 , Kurtosis, and ImpulseFactor.

Figure 13 shows the feature space constructed using eqn. (12) when considering both incipient and later-stage defects with a range of operating speeds and load condition. It can be seen that samples representing different groups are scattered and overlapped. This imposes difficulties in classification. For this reason, the intraclass transformation is applied to introduce clustering effects on the samples within each class.

7.4 Intraclass Transformation

The intraclass transformation is designed to increase the clustering of prototypes within the same class. This is realized through minimization of a metric between the points defining the class. For the k th class, there are a total of M_k prototypes, $\mathbf{y}_m^{(k)}$, each being a point in the two-dimensional feature space. The intraclass transform in the feature space is defined as:

$$\mathbf{y}'_{fm}{}^{(k)} = \mathbf{W}^{(k)} \mathbf{y}_{fm}^{(k)} \quad (14)$$

where the apostrophe indicates the result of the intraclass transformation. Denoting s_1^2 and s_2^2 as being the variances of the two variables in the feature space, $\mathbf{W}^{(k)}$ is defined by the following diagonal matrix

$$\mathbf{W}^{(k)} = \left(\frac{\mathbf{1}}{s_1^2} + \frac{\mathbf{1}}{s_2^2} \right) \cdot \mathbf{1} \begin{bmatrix} \frac{1}{s_1^2} & 0 \\ 0 & \frac{1}{s_2^2} \end{bmatrix} \quad (15)$$

Variances s_1^2 and s_2^2 are determined respectively by the first and second row of the following data matrix $\mathbf{Y}^{(k)}$ formed by M_k prototypes

$$\mathbf{Y}^{(k)} = \begin{bmatrix} y_{f11}^{(k)} & \cdots & y_{f1M_k}^{(k)} \\ y_{f21}^{(k)} & \cdots & y_{f2M_k}^{(k)} \end{bmatrix} \quad (16)$$

Through the intraclass transformation, the mean square intraset distance of the k th class is minimized (Andrews, 1972). It can be seen from eqn. (15) that the two coordinate dimensions are inversely proportional to the variance of their own dimension. This can be interpreted as stating that a small weight is to be given to those coordinates with large variances because these particular coordinates have little in common over the prototypes of the k th class. For those dimensions with near constant values, the variance is small, which implies large weighting. Figure 14 shows the effects of the intraclass transformation on the same set of data used to obtain Figure 13. Clearly, the samples belonging to the same class are clustered.

For bearing diagnostics, the vector \mathbf{x}_f , after the intraclass transformation, becomes

$$\mathbf{x}'_f = \mathbf{W} \mathbf{x}_f \quad (17)$$

where \mathbf{W} is defined in the same way as eqn. (15), except in this case, the variance will be determined based on \mathbf{x}_f spanning a number of samples.

7.5 Formation of Classification Space

Recall that the object of forming the classification space is to partition the feature space into K given regions, $S_1, \dots, S_k, \dots, S_K$. Mathematically, this problem lies in finding a function that can measure each point in the feature space in terms of its degree of membership to a given class. In pattern recognition, this function is called the discriminant function and is defined such that for all points \mathbf{x}_f in the feature space, within the region describing S_k , there exists a function $g_k(\mathbf{x})$ such that

$$g_k(\mathbf{x}_f) > g_j(\mathbf{x}_f) \quad \forall \mathbf{x}_f \in S_k \text{ and } \forall k \neq j \quad (18)$$

In other words, within the region S_k , the k th discriminant function will have the largest value.

The piecewise linear discriminant function is used, which can approximate the nonlinear boundaries separating the different class regions. This function is defined by the minimum distance between a point \mathbf{x}_f and the prototype points in class S_k .

$$d(\mathbf{x}_f, S_k) = \min_{m=1, \dots, M_k} \{d(\mathbf{x}_f, \mathbf{y}_{fm}^{(k)})\} \quad (19)$$

Point \mathbf{x}_f belongs to class S_k if the distance is minimum. The classification then becomes a task to determine the smallest distance between all of the prototypes of S_k and the unknown \mathbf{x}_f . Mathematically, this can be written as

$$\mathbf{x}_f \in S_k \text{ if } d(\mathbf{x}_f, S_k) = \min_k d(\mathbf{x}_f, S_k) \quad (20)$$

Through mathematical manipulation (Andrews, 1972), the piecewise linear discriminant function can be given as

$$g_k(\mathbf{x}_f) = \max_{m=1, \dots, M_k} \left\{ \mathbf{x}_f^T \mathbf{y}_{fm}^{(k)} - \frac{1}{2} \mathbf{y}_{fm}^{(k)T} \mathbf{y}_{fm}^{(k)} \right\} \quad (21)$$

The boundaries separating the different class regions are determined by the following equation

$$g_k(\mathbf{x}_f) - g_j(\mathbf{x}_f) = 0 \quad (22)$$

Figure 14 shows the boundaries determined by eqn. (19), illustrating very distinct partitioning of the space into a different class region for each bearing defect.

8 Bearing Diagnostics and Classification Based on One-Microphone Signals

The bearing conditions examined are given in the following table.

Table 4. Bearing Damage Conditions

Class	Symbol	Condition
C ₁	1	undamaged
C ₂	2	single spall on outer race
C ₃	3	multiple spall on outer race
C ₄	4	single spall on inner race
C ₅	5	multiple spall on inner race
C ₆	6	broken roller

Bearing diagnostics was carried out using a program written in MATLAB according to the computation procedure summarized in Figure 11. From the prototype data of the six classes, first the statistical parameters were calculated using eqns. (3)-(8). Each sample was then located in the feature space according to eqn. (12); this is shown in Figure 13. Through the intraclass transformation (eqn. (14)), the prototypes were then clustered in the feature space, as illustrated in Figure 14. Lastly, we constructed the six linear discriminant functions using eqn. (21) and determined the classification space, as shown in Figure 15.

To test the effectiveness of this method, we took a set of data with an unknown type of defect. We used our program and located the test data in the region of broken rollers, as shown in Figure 16 with a "+" symbol. The result was verified by checking the bearing, and it did, indeed, have a broken roller defect.

9 Combined Index Method Using Two-Microphone Signals

Figure 3 shows the two-microphone measurement system that is proposed in this paper for the diagnosis of tapered bearing defects. A linear model to calculate an index consisting of the two signals and their correlation is as follows:

$$I = W_1 A_1 + W_2 A_2 + W_3 C_{12} \quad (23)$$

where I denotes a defect index; A_1 and A_2 , represent the amplitudes at the defect frequency of microphone 1 and 2 signals respectively; C_{12} is the correlation coefficient of the two signals; and W_1 , W_2 , and W_3 are weighting factors.

For the purpose of bearing diagnostics, we want to obtain a distinct index value for each defect. In other words, we intend to use the proposed index as a descriptor to identify different defects.

The determination of A_1 , A_2 and C_{12} is straightforward. The first two can be obtained by the FFT and the third by correlation analysis. To ensure that we compare three variables with the same unit, they should all be normalized. Determination of the weighting factors is discussed in the following section.

9.1 Determination of Weighting Factors

For the purpose of increasing the clustering effect of each defect under different operating conditions, it is proposed here to use the intraclass transformation from pattern recognition to determine the weighting factors. In line with pattern recognition and prior to describing the intraclass transformation, we need to define the following vector representing the features under consideration.

$$\mathbf{x} = [x_1, \dots, x_i, \dots, x_n]^T \quad (24)$$

In this case, we consider three features, namely, $x_1 = A_1$, $x_2 = A_2$, and $x_3 = C_{12}$, and $n=3$.

The similarity of \mathbf{x} to the k th class can be measured by the following equation

$$S(x, \{(x_p^{(k)})_m\}) = \frac{1}{M_k} d^2(x, (x_p^{(k)})_m) \quad (25)$$

where S stands for the similarity measure, and d represents a distance function given as

$$d^2(\mathbf{x}, (\mathbf{x}_p^{(k)})_m) = \sum_{m=1}^{M_k} \sum_{i=1}^n (x_i - (x_i^{(k)})_m)^2 \quad (26)$$

The similarity measure given in eqn. (23) is an average of the squared distance between \mathbf{x} and the set of prototypes.

Assuming that a class is likely generated equally by each prototype for that class, the mean square intraset distance for the k th class can be given as

$$D_k^2 = \frac{1}{M_k(M_k - 1)} \sum_{l=1}^{M_k} \sum_{m=1}^{M_k} d^2((\mathbf{x}_p^{(k)})_l, (\mathbf{x}_p^{(k)})_m) \quad (27)$$

To minimize D_k^2 , meaning to increase the clustering effect of the prototypes under the same defect, weighting factors W_i are introduced to eqn. (27), that is

$$D_k^2 = \frac{1}{M_k(M_k - 1)} \sum_{l=1}^{M_k} \sum_{m=1}^{M_k} \sum_{i=1}^n W_i ((x_i^{(k)})_l - (x_i^{(k)})_m)^2 \quad (28)$$

Equation (28) can be considered as being equivalent to multiplying the feature vector by the diagonal matrix defined as $\text{diag}(W_i)$, which is referred to as the intraclass transformation. In this study we, in fact, define eqn. (23) as the dot product of the weighting factors with the feature vector

$$I = [W_1, W_2, W_3] \bullet [A_1, A_2, C_{12}]^T \quad (29)$$

For non-trivial solutions, constraint must be applied. There are two standard constraints. The first one is the constant sum

$$\sum_{i=1}^n W_i = 1 \quad (30)$$

and the second is the constant volume

$$\prod_{i=1}^n W_i = 1 \quad (31)$$

By using of the method of Lagrange multipliers, minimization of D_k^2 leads to the following weighting factors, for the constant sum

$$W_i = \frac{\left(\sum_{j=1}^n \frac{1}{s_j^2} \right)^{-1}}{s_i^2} \quad (32)$$

and for the volume constraint,

$$W_i = \frac{\left(\prod_{j=1}^n s_j \right)^{1/n}}{s_i} \quad (33)$$

where σ_i is the variance of the prototypes for the i th dimension of the feature vector.

The essence of the clustering is to bunch the prototypes of a class around their mean value. Since the variance represents the deviation from the mean value, dividing the feature vector by the variance, as in eqns. (32) and (33), will reduce the distance to the mean (i.e. increasing the clustering effect.) This, in turn, helps to create the distinct values of the proposed index for different defects.

In summary, the procedure to obtain the proposed index is as follows:

- select features;
- obtain prototypes of the selected features from measurement data samples;
- determine the variance for each dimension;
- determine the weighting factors and the index.

10 Bearing Diagnosis Using Combined Index Method

This method has been employed to diagnose the defects of the tapered roller bearings from the data obtained from the laboratory tests. As in the previous analysis based on one-microphone measurements, analysis was done on the data from two types of railway bearings, F (under loads of 8K lb. and 33K lb.) and E (8K and 27.5K lb.), and at speeds ranging from 30 mph to 80 mph.

10.1 Prototype Data Processing

The combined index method was used to process the prototype data for the purpose of establishing the relationship between the values of the index and the different bearing defects. Five classes were considered, including the good bearing, and the bearings with single cone (inner race) spall, single cup (outer race) spall, multiple cup spall, and broken roller.

10.2 Weighting Factors Considering Speed Variation

FFT and correlation analyses for each defect class were performed to generate the prototype data, with the results for different speeds given in Tables 5 to 9. Note that in the case of the good bearing, we select A_1 and A_2 at the shaft rotation frequency, as there is no defect frequency. For the defect bearings, we select A_1 and A_2 at the analytical defect frequency. For each of the five defect classes given in Tables 5-9, we calculate their respective weighting factors. To do this, first we calculate the variance of column values in each table, and then the weighting factors using eqn. (28). Table 10 lists the weighting factors for the five defect cases under the constant sum constraint.

Table 5. Prototype for Good Bearing

Speed (mph)	A_1	A_2	C_{12}
30	0.0541	8.93	0.34
40	0.0477	7.78	0.63
50	0.018	0.5025	0.72
60	0.0179	3.33	0.67
70	0.031	3.97	0.65
80	0.0089	5.938	0.66

Table 6. Prototypes for the Single Cone Spall

Speed (mph)	A_1	A_2	C_{12}
30	0.077	0.99	0.57
40	0.126	1.097	0.39
50	0.214	0.43	0.55
60	0.455	0.825	0.55
70	0.235	1.333	0.55
80	0.497	0.8735	0.43

Table 7. Prototypes for the Single Cup Spall

Speed (mph)	A_1	A_2	C_{12}
30	0.0865	0.8734	0.7
40	0.1283	0.9411	0.76
50	0.2775	0.3343	0.8
60	0.197	0.2447	0.81
70	0.2254	0.283	0.8
80	0.3376	0.249	0.82

Table 8. Prototypes for the Multiple Cup Spall

Speed (mph)	A_1	A_2	C_{12}
30	0.125	0.2481	0.86
40	0.2556	0.2759	0.76
50	0.2394	0.18	0.79
60	0.51	0.17	0.82
70	0.0878	0.06	0.84
80	0.0953	0.0375	0.82

Table 9. Prototypes for the Broken Rollers

Speed (mph)	A_1	A_2	C_{12}
30	0.0637	2.592	0.53
40	0.1132	1.4798	0.62
50	0.1673	2.6274	0.72
60	0.1374	1.0491	0.67
70	0.1852	1.0115	0.65
80	0.1852	1.1037	0.67

Table 10. Weighting Factor under the Constant Sum Constraint

Class	W_1	W_2	W_3
Good condition	0.9828	0.0000	0.0172
Single cone spall	0.1563	0.0502	0.7935
Single cup spall	0.1865	0.015	0.7984
Multiple cup spall	0.0423	0.1008	0.8568
Broken roller	0.6445	0.0025	0.353

By using the weighting factors, the index for each defect class of bearing under different speeds is determined with the results presented in Figure 3.

It can be seen from Figure 17 that the values of the index determined from the constant sum constraint fall into distinct ranges for different defects. This gives rise to the possibility of using this index for bearing diagnostics. The good bearing has values within the range of 0-1, which is clearly separated from other defect classes. The broken roller has values within the range of 2-3.5; the single cone spall class within the range of 3.5-5.5; the single cup spall within the range of 5.6-7.5; and the multiple cup spall within the range of 6.5-7.5. There is some overlapping between the different defect classes, as shown in Figure 18. Further study is needed to establish clearly distinct indexes for bearing fault diagnosis.

For comparison purposes, we also tried the constant volume constraint to determine the weighting factors. However, as illustrated in Figure 19, this constraint does not give as distinct a classification as the constant sum constraint.

10.3 Weighting Factors Considering Loading Variation

On the test rig, two loading conditions were examined: 8K lb. and 27.5K lb. simulating 70 and 100 ton freight car capacities. The prototypes presented in Tables 5-9 were obtained under 27.5K lb. To consider the effects of load variation, the prototypes were obtained for 8K lb. for the same speed range, 30 to 80 mph, and they were added to Tables 5-9 to form augmented prototypes. The resulting weighting factors are listed in the Table 11, and the resulting index for each defect class under the different speeds and loads is shown in Figure 20.

A different approach is tried based on the covariance between the two prototypes under the two different loading conditions. Table 12 lists the weighting factors and Figure 21 shows the index. A difference in the two approaches is not obvious.

Table 11. Weighting Factors Considering Two Different Loading Conditions

Class	W_1	W_2	W_3
Good condition	0.9856	0.0000	0.0143
Single cone spall	0.1794	0.0261	0.7945
Single cup spall	0.1820	0.0235	0.7946
Multiple cup spall	0.0506	0.1178	0.8316
Broken roller	0.4681	0.0035	0.5285

Table 12. Weighting Factors Based on the Covariance of Two Loading Conditions

Class	W_1	W_2	W_3
Good condition	0.9977	0.0000	0.0024
Single cone spall	0.2472	0.0467	0.7061
Single cup spall	0.2678	0.1625	0.5697
Multiple cup spall	1.1063	-0.046	-0.06
Broken roller	0.729	0.0214	0.2496

10.4 Graphic User Interface

A graphic user interface based on the combined index method has been developed and described in the accompanying report (Reference.) This interface provides the capability to capture microphone signals and store these signals in ASCII or binary files. The user can then perform individual statistical and signal analysis functions on the acoustic data or run it through a bearing diagnostics algorithm. The bearing diagnosis will highlight the most likely defect exhibited by that bearing. Figure 22 illustrates the user's front panel when performing bearing diagnostics.

11. Conclusions

Bearing diagnostic methods based on pattern recognition of statistical parameters were investigated.

Based on one-microphone signals, using a combination of bearing energy and impulse parameters, a pattern recognition technique to classify and identify six commonly occurring freight car bearing defects was developed. Two-dimensional feature space was selected to classify the defects. The pattern recognition technique was tested, and it successfully identified an unknown (mystery) defect.

For diagnosing roller, railway bearings, the combined index method was developed to process the signals from a two-microphone arrangement. The idea was introduced to use the intraclass transformation to determine the weighting factors through a clustering effect. Both speed and loading variations were considered. Based on the constant sum constraint, the determined indexes are effective for identifying the bearing defects with a variation of speeds under constant loading. A graphic user interface system based on this method was developed.

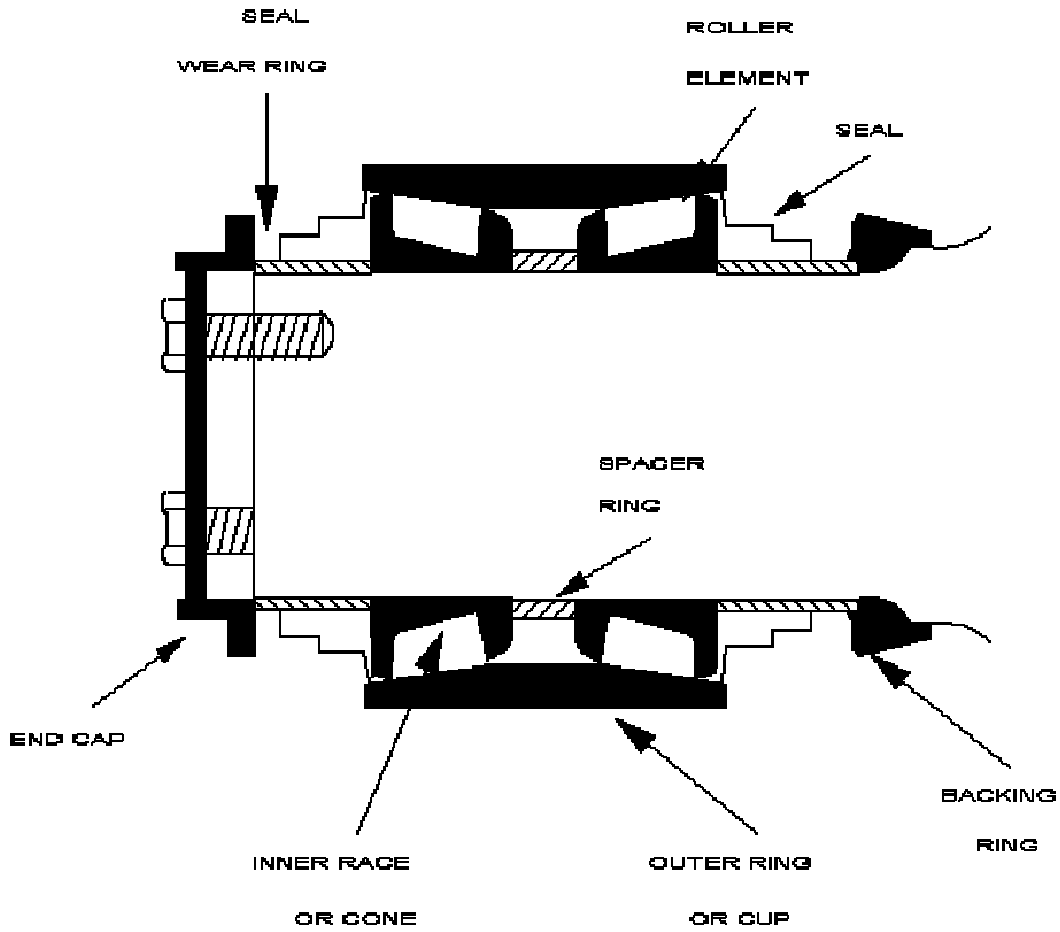


Figure 1: Freight Car Bearing Assembly

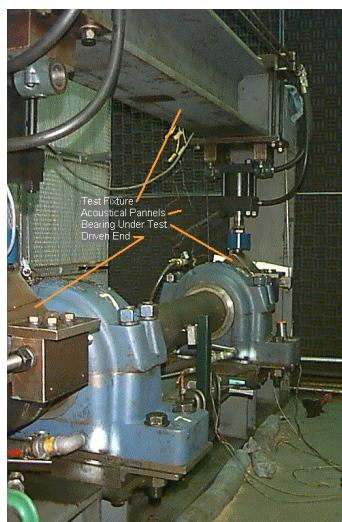


Figure 2: Bearing Test Rig

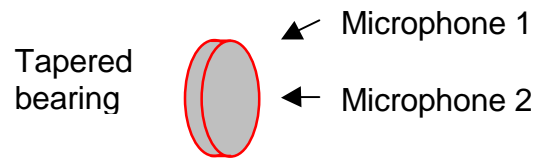


Figure 3: Two-microphone Measurement System

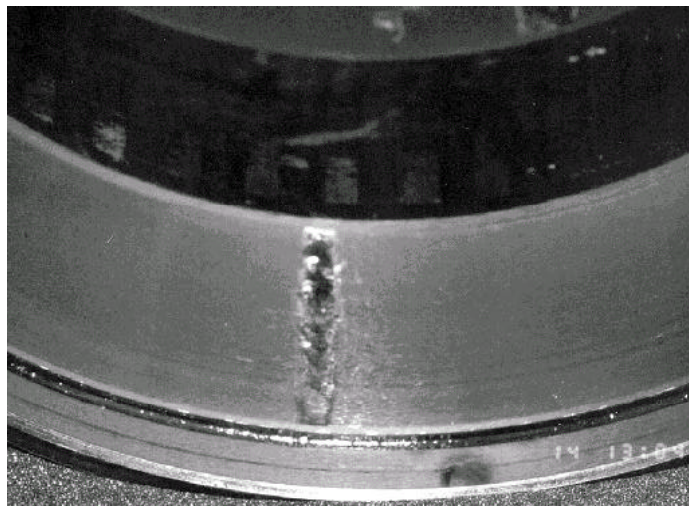


Figure 4: Single Cup Spall



Figure 5: Multiple Cone (inner race) Spalling



Figure 6: Water Etching



Figure 7: Multiple Cup (outer race) Spalling



Figure 8: Broken Roller

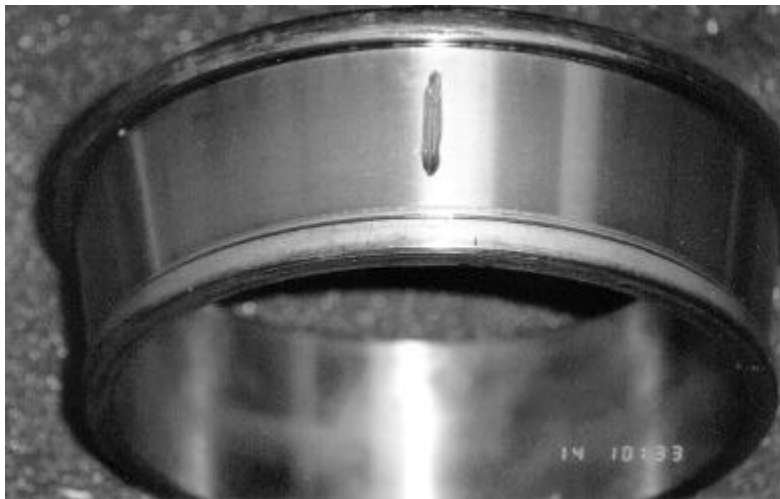


Figure 9: Single Cone Spall

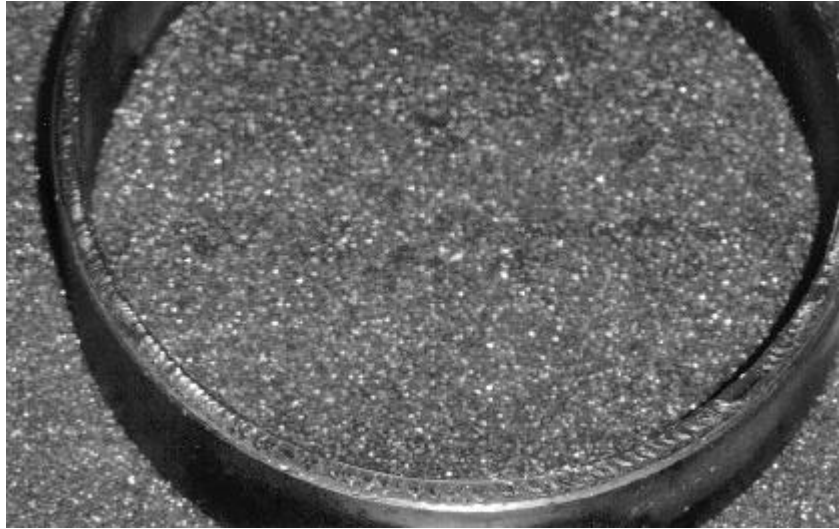


Figure 10: Spun Cone

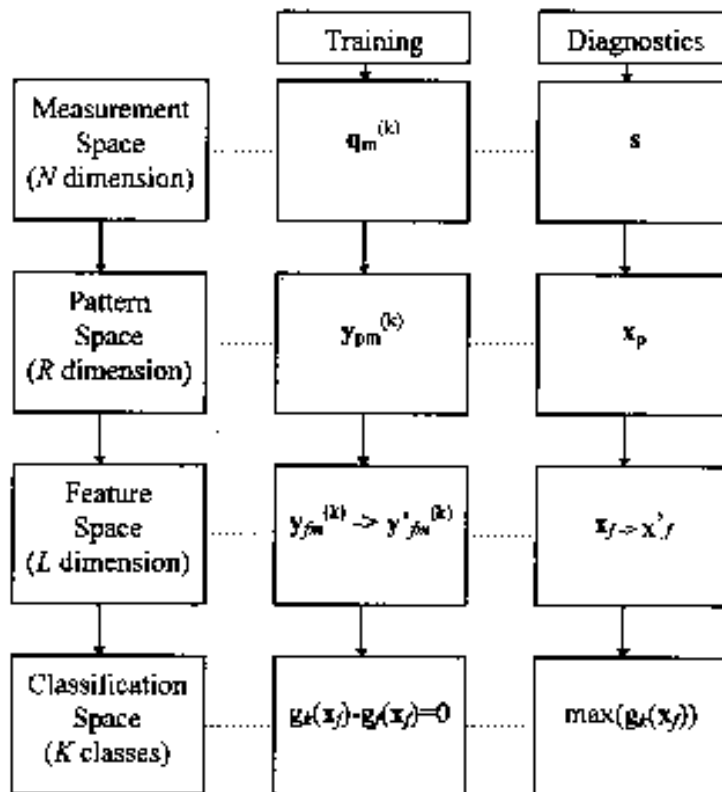


Figure 11: Mathematical Transformations of Four Spaces

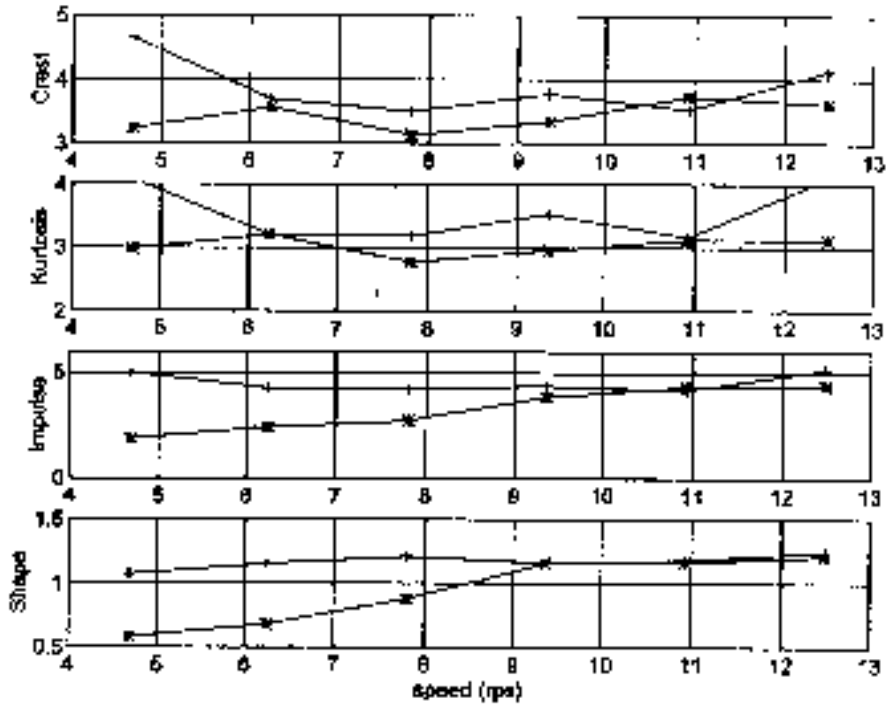


Figure 12(a): Variation of the Four Parameters, z_3 to z_6 , with Speed for Light Loading.

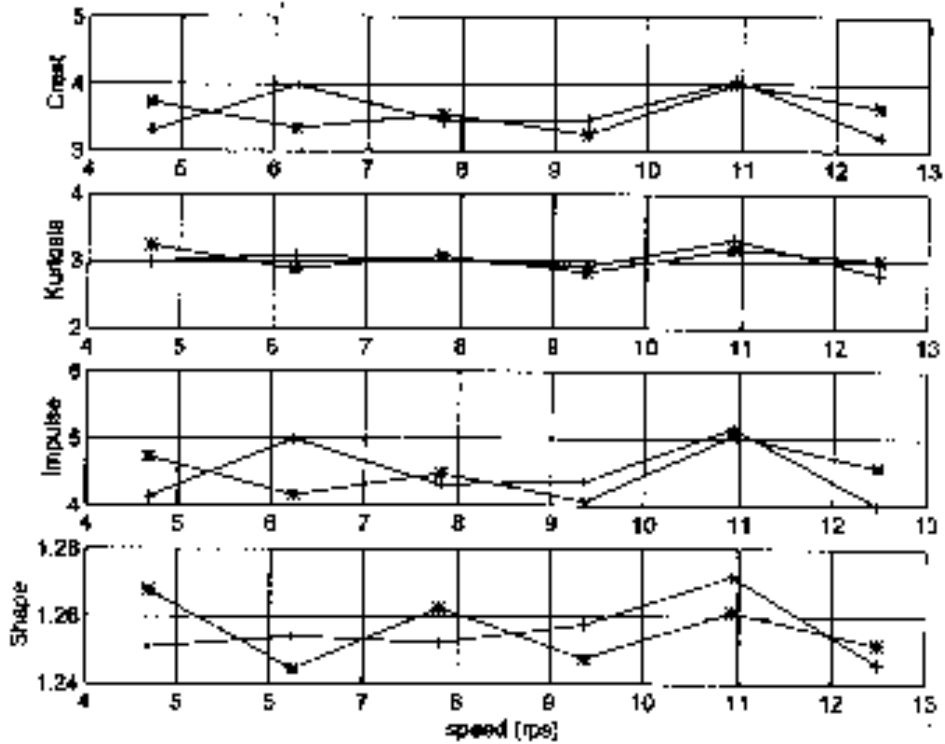


Figure 12(b): Variation of the Four Parameters with Heavy Loading.

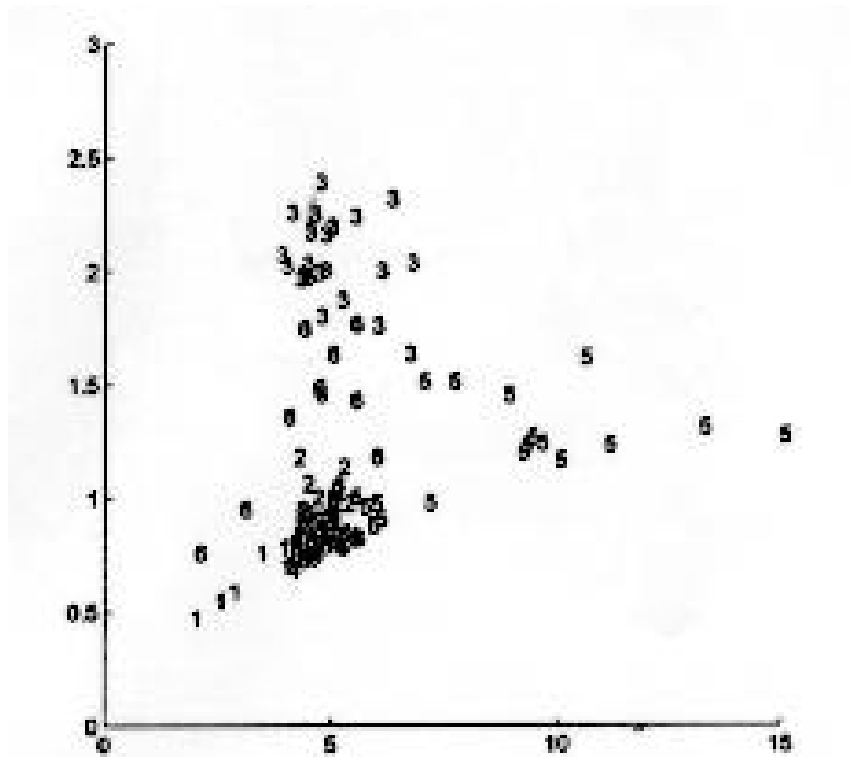


Figure 13: Feature Space without Intraclass Transformation

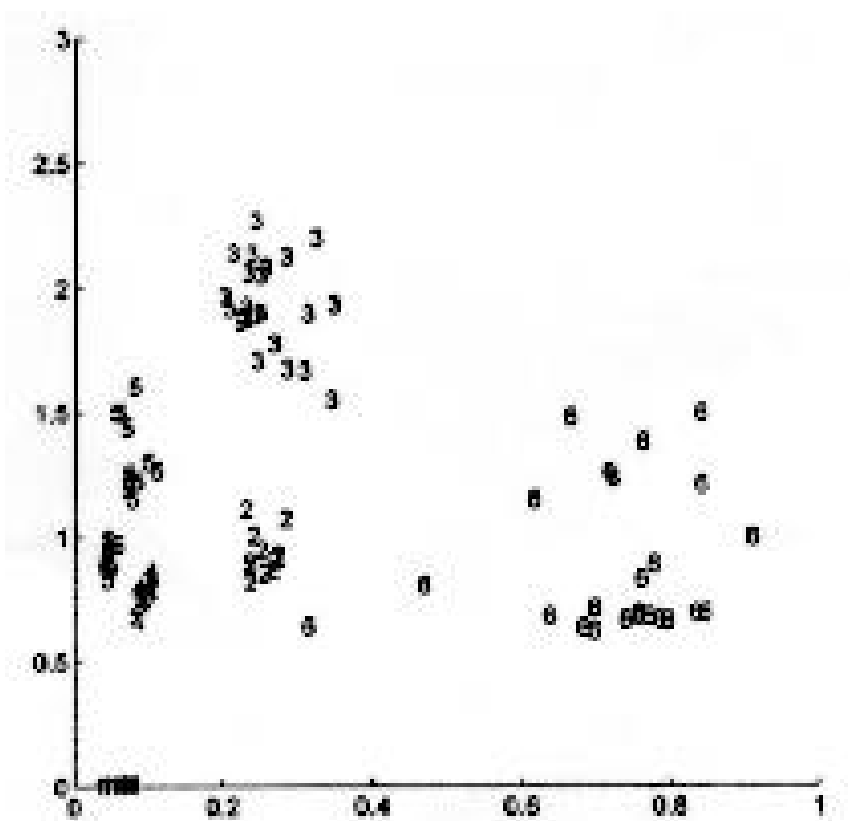


Figure 14: Feature Space with Intraclass Transformation

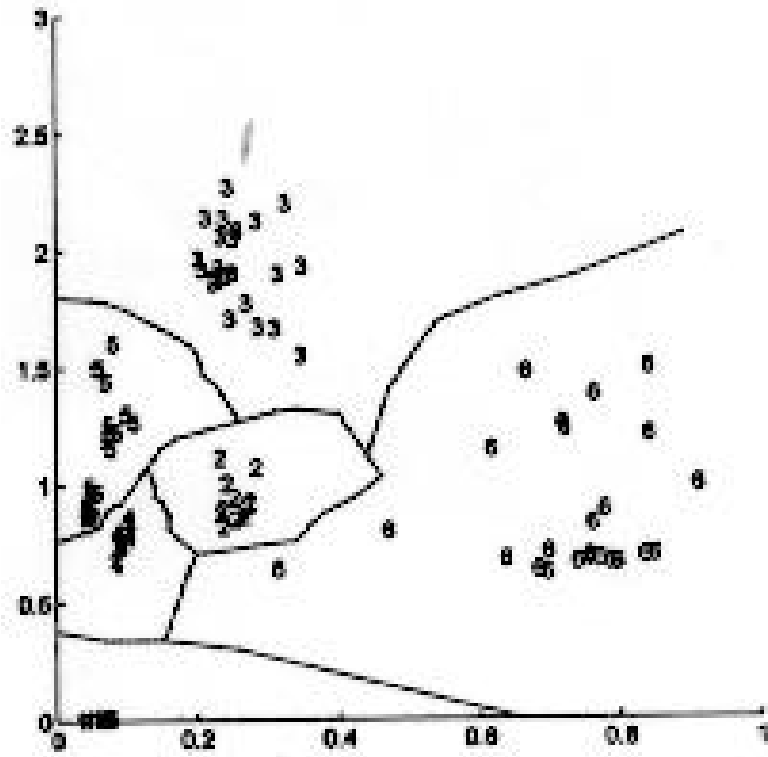


Figure 15: Classification Space

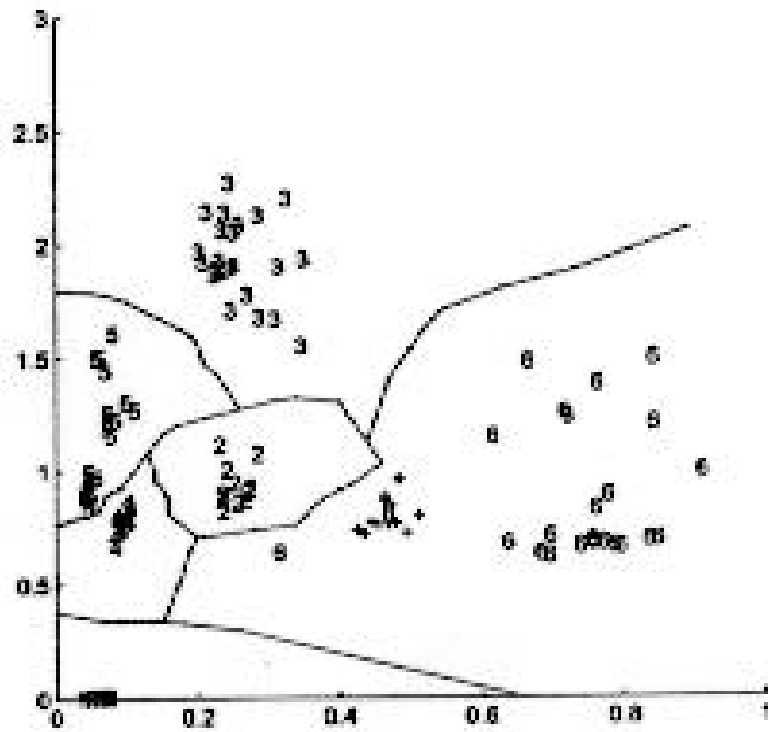


Figure 16: Identification of Unknown Bearing Fault

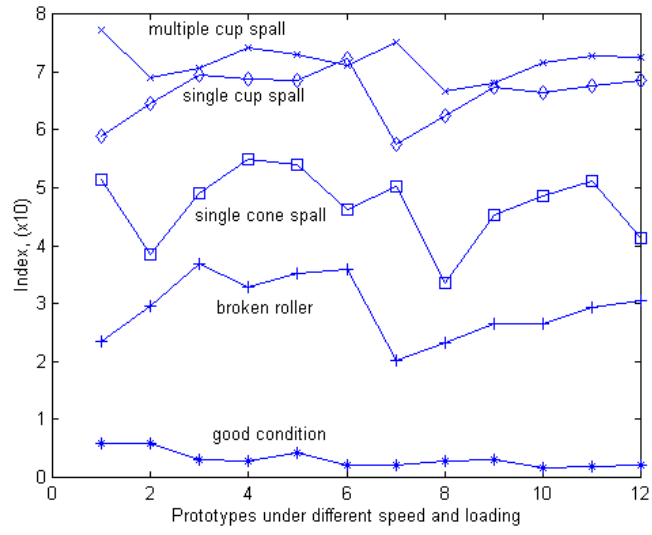


Figure 17: Index of Different Defect Classes under the Constant Sum Constraint

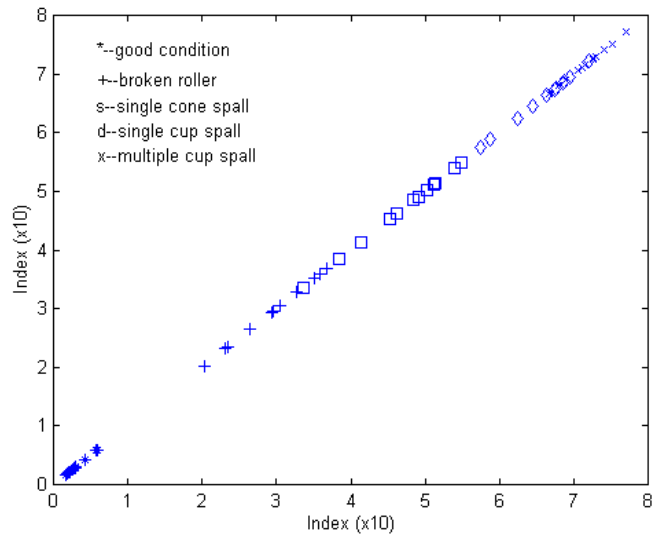


Figure 18: Index Overlapping between Different Defect Classes

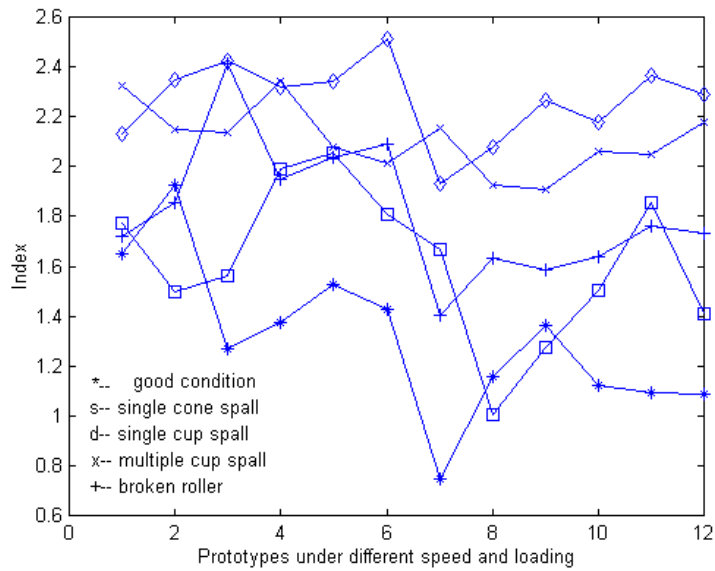


Figure 19: Index of Different Defect Classes under the Volume Constraint

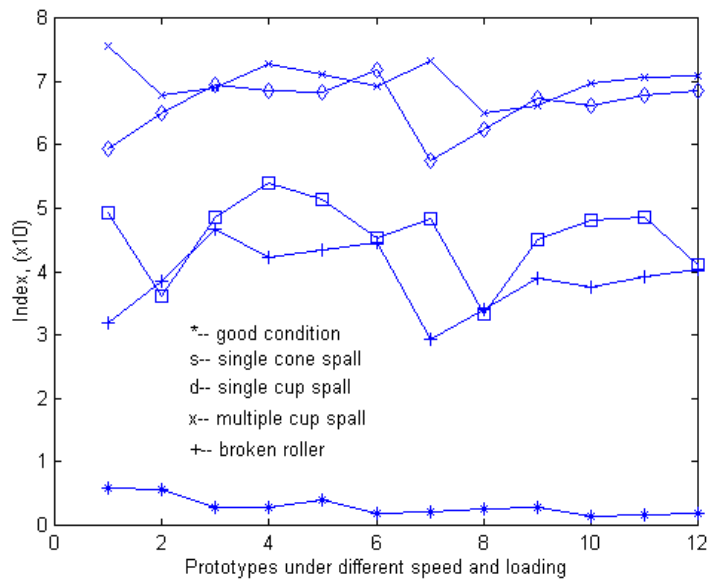


Figure 20: Index of Different Defect Classes Considering Two Loading Conditions

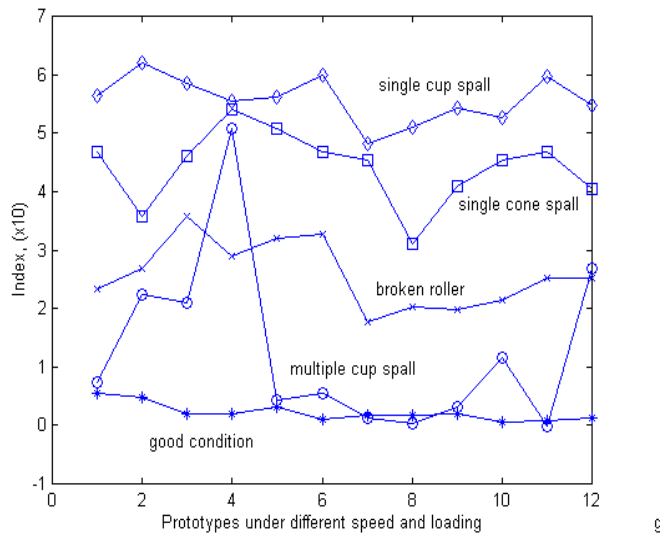


Figure 21: Index of Different Defect Classes Based on the Covariance of Two Loading Conditions

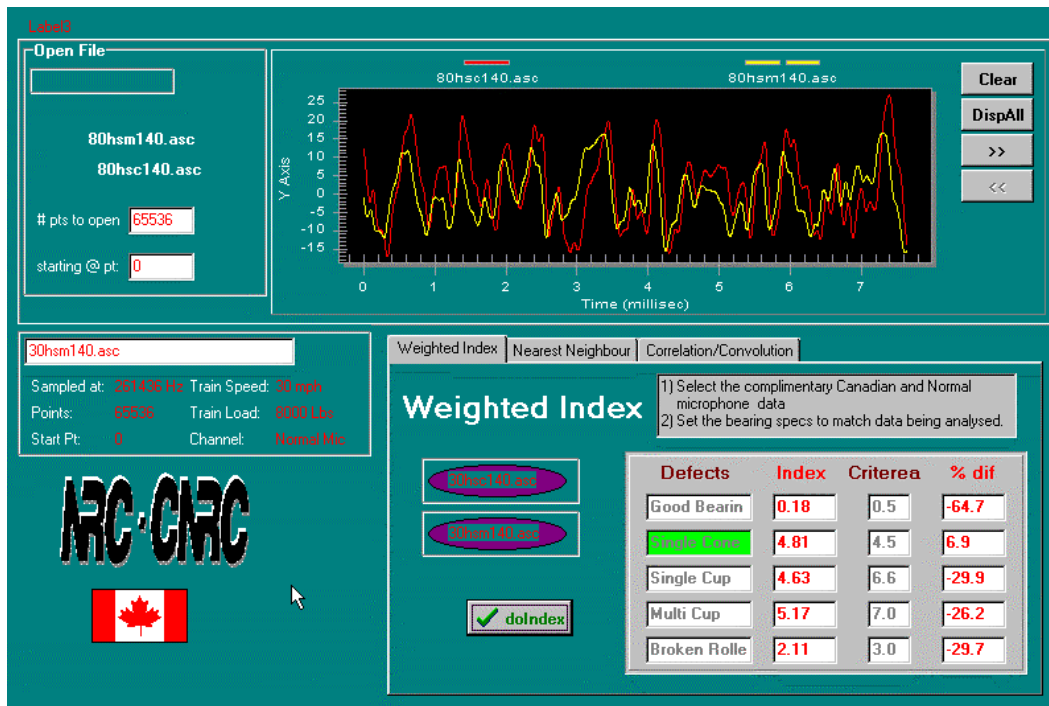


Figure 22: Picture of the Developed Software

13.0 References

Andrews, H.C., 1972, *Mathematical Techniques in Pattern Recognition*, Wiley-Interscience.

Braun, S., 1986, *Mechanical Signature Analysis*, Academic Press.

McFadden, P.D. and Smith, J.D., 1984a, "Model for the Vibration Produced by a Single Point Defect in a Rolling Element Bearing", *Journal of Sound and Vibration*, Vol. 996, No. 1, 1984, pp. 69-82.

McFadden, P.D. and Smith, J.D., 1984b, "Model for the Vibration Produced by Multiple Point Defects in a Rolling Element Bearing", *Journal of Sound and Vibration*, Vol. 996, No. 2, 1985, pp. 263-273.

Howard, I., 1994, "A Review of Rolling Element Bearing Vibration – Detection, Diagnosis and Prognosis", Defense Science and Technology Organization, Australia.

Rao, B.K.N., 1996, *Handbook of Condition Monitoring*, Elsevier Advanced Technology, Oxford.

Appendix A: Test Set-Up and Instrumentation

Experimental Conditions

Load on Bearings (K lbs.)	8 (class E & F), 27 (class E), 33 (class F)
Speeds (mph)	25, 30, 40, 50, 60, 70, 80

Bearing Class E

Size (inches)	6 x 11
# of Rollers (N)	24
Roller Length (inches)	1.55720
Roller Diameter (inches)	0.70470
Roller Pitch Diameter (inches)	7.09460
Cone Bore Diameter (inches)	5.68700
Cup Outside Diameter (inches)	8.68750
Bearing Width (inches)	6.12500
1/2 Included Cup Angle (deg)	10
Standard Wheel Diameter (inches)	35.89

Bearing Class F

Size (inches)	6 1/2 x 12
# of Rollers (N)	23
Roller Diameter (inches)	0.84235
Roller Pitch Diameter (inches)	7.99057
Cone Bore Diameter (inches)	6.18700
Cup Outside Diameter (inches)	9.93750
Bearing Width (inches)	7.00000
1/2 Included Cup Angle (deg)	10
Standard Wheel Diameter	35.89

Instrumentation (typical values)

Number of data points:	522875
Digitization rate (Hz)	261436
Data sampling duration (sec)	2.000